

Parasitic small-moment-antiferromagnetism and non-linear coupling of hidden order and antiferromagnetism in URu₂Si₂ observed by Larmor diffraction

P. G. Niklowitz,^{1,2} C. Pfleiderer,¹ T. Keller,^{3,4} M. Vojta,⁵ Y.-K. Huang,⁶ and J. A. Mydosh⁷

¹Physik Department E21, Technische Universität München, 85748 Garching, Germany

²Department of Physics, Royal Holloway, University of London, Egham TW20 0EX, UK

³ZWE FRM II, Technische Universität München, 85748 Garching, Germany

⁴Max-Planck-Institut für Festkörperforschung, Heisenbergstrasse 1, 70569 Stuttgart, Germany

⁵Institute for Theoretical Physics Universität zu Köln, Zùlpicher Strasse 77, 50937 Köln, Germany

⁶Van der Waals-Zeeman Institute, University of Amsterdam, 1018XE Amsterdam, The Netherlands

⁷Kamerlingh Onnes Laboratory, Leiden University, 2300RA Leiden, The Netherlands

We report simultaneous measurements of the distribution of lattice constants and the antiferromagnetic moment in high-purity URu₂Si₂, using both Larmor and conventional neutron diffraction, as a function of temperature and pressure up to 18 kbar. We establish that the tiny moment in the hidden order (HO) state is purely parasitic and quantitatively originates from the distribution of lattice constants. Moreover, the HO and large-moment antiferromagnetism (LMAF) at high pressure are separated by a line of first-order phase transitions, which ends in a bicritical point. Thus the HO and LMAF are coupled non-linearly and must have different symmetry, as expected of the HO being, e.g., incommensurate orbital currents, helicity order, or multipolar order.

PACS numbers: 61.05.F-;62.50.-p;71.27.+a;75.30.Kz

Keywords: hidden order, antiferromagnetism, Larmor diffraction, pressure, neutron diffraction

In recent years hydrostatic pressure has become widely used in the search for new forms of electronic order, because it is believed to represent a controlled and clean tuning technique. Novel states discovered in high-pressure studies include superconducting phases at the border of magnetism and candidates for genuine non-Fermi liquid metallic states. However, a major uncertainty in these studies concerns the possible role of pressure inhomogeneities, that originate, for instance, in the pressure-transmitting medium and inhomogeneities of the samples. To settle this issue requires microscopic measurements of the distribution of lattice constants across the entire sample volume, which, to the best of our knowledge, has not been available so far.

The perhaps most prominent and controversial example that highlights the importance of sample inhomogeneities and pressure tuning is the heavy-fermion superconductor URu₂Si₂. The reduction of entropy at a phase transition at $T_0 \approx 17.5$ K, discovered in URu₂Si₂ over twenty years ago, is still not explained [1, 2, 3]. The associated state in turn is known as ‘hidden order’ (HO). The discovery of the HO was soon followed by the observation of a small antiferromagnetic moment (SMAF), $m_s \approx 0.01 - 0.04 \mu_B$ per U atom [4] then believed to be an intrinsic property of the HO. The emergence of large-moment antiferromagnetism (LMAF) of $m_s \approx 0.4 \mu_B$ per U atom [5] under pressure consequently prompted intense theoretical efforts to connect the LMAF with the SMAF and the HO. In particular, models have been proposed that are based on competing order parameters of the *same* symmetry, i.e., linearly coupled order parameters, in which the SMAF is intrinsic to the HO [6, 7, 8, 9]. This is contrasted by proposals for the HO parameter

such as incommensurate orbital currents [10], multipolar order [11], or helicity order [12], where HO and LMAF break *different* symmetries.

The symmetry relationship of HO and LMAF clearly yields the key to unravelling the nature of the HO state [8, 9]. While some neutron scattering studies of the temperature–pressure phase diagram suggest that the HO–LMAF phase boundary ends in a critical end point [13], other studies concluded that it meets the boundaries of HO and LMAF in a bicritical point [14, 15, 16, 17]. This distinction is crucial, as a critical end point (bicritical point) implies that HO and LMAF have the same (different) symmetries, respectively [9]. Moreover, there is a substantial disagreement w.r.t. the location and shape of the HO–LMAF phase boundary (see e.g. Ref. [18]). This lack of consistency is, finally, accompanied by considerable variations of the size and pressure dependence of the moment reported for the SMAF [18], where NMR studies in powder samples suggested the SMAF to be parasitic [19]. Accordingly, to identify the HO in URu₂Si₂ it is essential to clarify unambiguously the nature of the SMAF and the symmetry relationship of HO and LMAF.

It was long suspected that the conflicting results are due to a distribution of lattice distortions due to defects. Notably, uniaxial stress studies showed that LMAF is stabilized if the c/a ratio η of the tetragonal crystal is reduced by the small amount $\Delta\eta_c/\eta \approx 5 \cdot 10^{-4}$ [20]. Hence, the parasitic SMAF may in principle result from a distribution of η values across the sample, with its magnitude depending on sample quality and experimental conditions. In particular, differences of compressibility of wires, samples supports or strain gauges that are welded, glued or soldered to the samples will

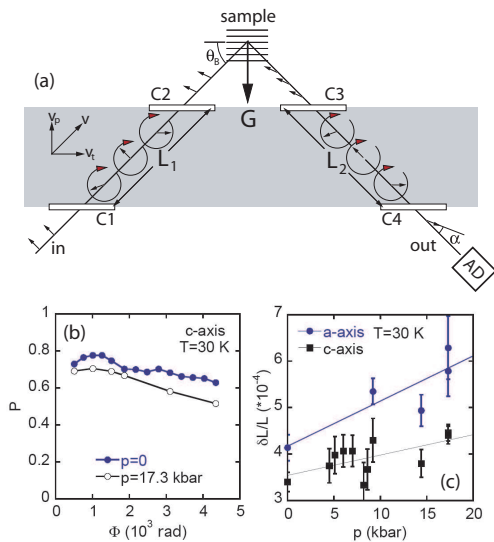


FIG. 1: (a) Schematic of Larmor diffraction [22, 23], see text for details. (b) Typical variation of the polarization P as a function of the total Larmor phase Φ . (c) Pressure dependence of the width of the lattice-constant distribution for the a - and c -axis in URu_2Si_2 . With increasing pressure the width of the distribution increases.

forcibly generate uncontrolled local strains that strongly affect any conclusions about the SMAF signal (see, e.g., Refs [14, 15, 16, 17]).

In this Letter we report simultaneous measurements of the distribution and temperature dependence of the lattice constants, as well as the antiferromagnetic moment, of a pure single crystal of URu_2Si_2 utilizing a novel neutron scattering technique called Larmor diffraction (LD). This allowed to study samples that are completely free to float in the pressure transmitting medium, thereby experiencing essentially ideal hydrostatic conditions at high pressures. Our data of the distribution of lattice constants $f(\Delta\eta/\eta)$ establishes *quantitatively* that the SMAF is purely parasitic. In addition, we find a rather abrupt transition from HO to LMAF which extends from $T=0$ up to a bicritical point (preliminary data of $T_N(p)$ were reported in [21]). We conclude that the HO–LMAF transition is of first order and that HO and LMAF must be coupled non-linearly. This settles the perhaps most important, long-standing experimental issue on the route to identifying the HO.

Larmor diffraction permits high-intensity measurements of lattice constants with an unprecedented high resolution of $\Delta a/a \approx 10^{-6}$ [22, 23]. As shown in Fig. 1 (a) the sample is thereby illuminated by a polarized neutron beam (arrows indicate the polarization); G is the reciprocal lattice vector; θ_B is the Bragg angle; AD is the polarization analyzer and detector. The radio frequency (RF) spin resonance coils (C1–C4) change the polarization direction, as if the neutrons undergo a Larmor precession with frequency ω_L along the distance $L = L_1 + L_2$. The

total Larmor phase of precession Φ thereby depends linearly on the lattice constant a : $\Phi = 2\omega_L L m a / (\pi \hbar)$ (m is the mass of the neutron [22, 23]).

The Larmor diffraction was carried out at the spectrometer TRISP at the neutron source FRM II. The temperature and pressure dependence of the lattice constants was inferred from the (400) Bragg peak for the a axis and the (008) Bragg peak for the c axis. The magnetic ordered moment was monitored with the same setup using conventional diffraction. For our high-pressure studies a Cu:Be clamp cell was used with a Fluorinert mixture [24]. The pressure was inferred at low temperatures from the (002) reflection of graphite as well as absolute changes of the lattice constants of URu_2Si_2 taking into account published values of the compressibility.

The single crystal studied was grown by means of an optical floating-zone technique at the Amsterdam/Leiden Center. High sample quality was confirmed via X-ray diffraction and detailed electron probe microanalysis. Samples cut-off from the ingot showed good resistance ratios (20 for the c axis and ≈ 10 for the a axis) and a high superconducting transition temperature $T_c \approx 1.5$ K. The magnetization of the large single crystal agreed very well with data shown in Ref. [25] and confirmed the absence of ferromagnetic inclusions. Most importantly, in our neutron scattering measurements we found an antiferromagnetic moment $m_s \approx 0.012 \mu_B$ per U atom, which matches the smallest moment reported so far [18].

As the Larmor phase Φ is proportional to the lattice constant a , the polarization P of the scattered neutron beam reflects the distribution of lattice constants *across the entire sample volume* [23]. While Larmor diffraction was recently employed for the first time in a high-pressure study [26], measurements of the distribution of lattice have not been exploited to resolve a major scientific issue (for proof of principle studies in Al-alloys see Ref. [22]).

In order to explore the origin of the SMAF moment we have measured the spread of lattice constants, keeping in mind that a distribution of the c/a lattice-constant ratio η may be responsible for AF order in parts of the sample. As shown in Fig. 1 (b) $P(\Phi)$ changes only weakly between ambient pressure and 17.3 kbar. Accordingly the distribution of lattice constants, which is given by the Fourier transform of $P(\Phi)$, changes only weakly as a function pressure as shown in Fig. 1(c). Thus pressure only slightly boosts the distribution of lattice constants, but does not generate substantial additional inhomogeneities. Moreover, we confirmed that the size of m_s remained unchanged tiny after our high-pressure studies.

Assuming a Gaussian distribution of both lattice constants, we infer the distribution of η . At low pressure, we arrive at a full width at half-maximum of $f(\Delta\eta/\eta)_{\text{FWHM}} \approx 3.8 \cdot 10^{-4}$. Recalling that the tail of the Gaussian distribution beyond $\Delta\eta_c/\eta \approx 5 \cdot 10^{-4}$ represents the sample's volume fraction in which LMAF forms [20], an average magnetic moment of $0.015(5)\mu_B$ is expected in

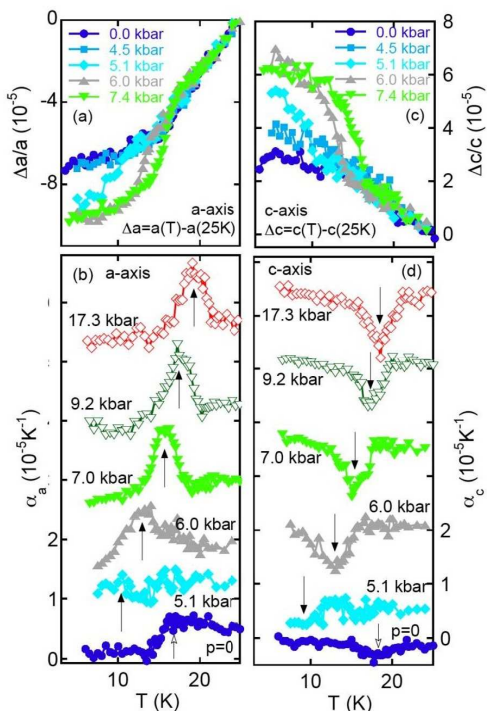


FIG. 2: Temperature dependence of the lattice constants and thermal expansion at various pressures. The HO and LMAF transitions are indicated by empty and filled arrows, respectively. (a) Data for the a -axis; (b) thermal expansion of the a -axis derived from the data shown in (a). (c) Data for the c -axis; (d) thermal expansion of the c -axis derived from the data shown in (c).

our sample. This is in excellent quantitative agreement with the experimental value and represents the first main result we report.

We continue with a discussion of the temperature dependence of the lattice constants and its change with pressure. At zero pressure in a wide temperature range below room temperature (not shown) the thermal expansion is positive for both axes [27]. However, for the c -axis, the lattice constant shows a minimum close to 40 K and turns negative at lower temperatures. This general behavior is unchanged under pressure.

Shown in Fig. 2 are typical low-temperature data for the a - and c -axis. At ambient pressure T_0 can be barely resolved. However, when crossing $p_c \approx 4.5$ kbar a pronounced additional signature emerges rapidly and merges with T_0 . Measurements of the antiferromagnetic moment (see below), identify this anomaly as the onset of the LMAF order below its T_N . At the transition the lattice constant for the a - and c -axis show a pronounced contraction and expansion, respectively.

The pressure and temperature dependence of m_s determined at (100) is shown in the inset of Fig. 3 (a). Close to $p_c \approx 4.5$ kbar, where T_N is near base temperature, we observe first evidence of the LMAF magnetic signal, which

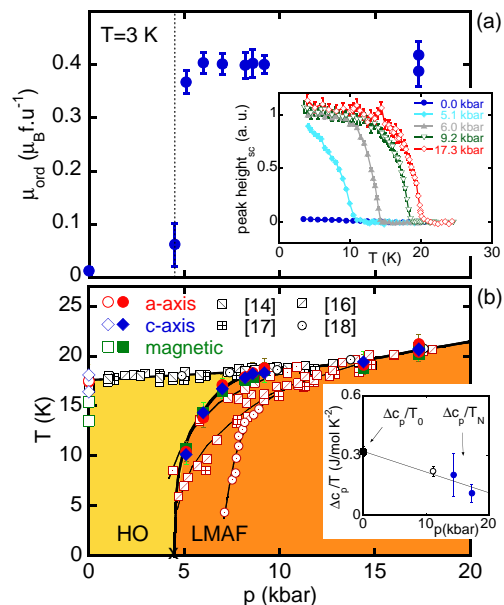


FIG. 3: (a) Pressure dependence of the low-temperature magnetic moment. The inset shows the temperature dependence of the magnetic peak height at various pressures. (b) Phase diagram based on Larmor diffraction and conventional magnetic diffraction data. The onset of LMAF is marked by full and of HO by empty symbols (x marks a transition near base temperature). For better comparison data of T_N (black symbols) from Refs. [14, 16, 17, 18] are shown. The T_0 values (red symbols) of all references are consistent. Inset: background-free specific-heat jump derived from thermal-expansion data via the Ehrenfest relation (full circles). Heat capacity data is taken from Refs. 1 (square) and 16 (empty circle).

rises steeply and already reaches almost its high-pressure limit at 5 kbar. The pressure dependence was determined by assuming the widely reported high-pressure value of $m_s = 0.4\mu_B$ and comparing the magnetic (100) and nuclear (004) peak intensity.

The temperature–pressure phase diagram shown in Fig. 3 (b) displays T_0 and T_N taken from the magnetic Bragg peak (Fig. 3 (a)) and from the Larmor diffraction data (Fig. 2), respectively. The different data sets show excellent agreement (except at $p = 0$, due to the variable parasitic nature of the SMAF). The main results contained in Fig. 3 are (i) the very small value of $0.012 \mu_B$ of the average low-temperature ordered moment at zero pressure, (ii) a particularly abrupt increase of the low-temperature moment at $p_c \approx 4.5$ kbar (as compared to previous studies [14, 15, 16, 17, 18]), (iii) the steep slope of the HO–LMAF phase boundary, and (iv) the merging of the HO–LMAF phase boundary with the T_0 transition lines at approximately 9 kbar. Fig. 2 (b) shows that we can follow this phase boundary from low T up to T_0 .

Most importantly, (iv) implies that HO and LMAF are fully separated by a phase boundary which has to be of first order with a bicritical point, since three second-order phase transition lines cannot meet in one point. (Note

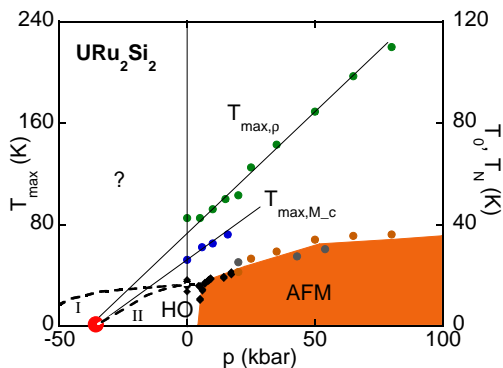


FIG. 4: Extended phase diagram of URu_2Si_2 based on the data presented here (diamonds) and signatures in resistivity (brown[28] and grey[16] circles). $T_{\max,\rho}$ and T_{\max,M_c} denote coherence maxima in the resistivity [28] and magnetisation [25], respectively. The HO might either mask a QCP (I) or replace LMAF (II) near quantum criticality.

that the phase boundaries from the HO and LMAF to the disordered high-temperature phase are already known to be of second order from qualitative heat capacity measurements [1, 16].) This conclusion is perfectly consistent with (ii) and (iii), and it excludes a linear coupling between the HO and LMAF order parameters [9].

Although our results show that the HO and LMAF must have different symmetry, they also suggest that both types of order may have a common origin. Using the Ehrenfest relation, we have converted our thermal expansion data into a background-free estimate of the specific-heat jump, ΔC , at the PM to LMAF transition. The inset in Fig. 3 (b) shows a continuous evolution with pressure of the jumps at the LMAF to PM and corresponding HO to PM transitions. The common origin of both phases may in fact be related to excitations seen in neutron scattering. Notably, excitations at (1,0,0) only appear in the HO phase and may be its salient property [29, 30]. However, excitations at (1.4,0,0) in the PM state become gapped in both the HO and LMAF state and have been quantitatively linked to the specific heat jump at zero pressure [31].

Finally, Fig. 4 suggests a new route to the HO. It shows a summary of the pressure evolution of features in the resistivity and magnetization, which suggest the existence of an AF quantum critical point (QCP) at an extrapolated negative pressure. Remarkably, these features, which are usually denoted as Kondo or coherence temperature, all seem to extrapolate to the same critical pressure. The HO in URu_2Si_2 could be understood as emerging from quantum criticality, possibly even masking an AF QCP (case I in Fig. 4). However, considering the remoteness of the proposed QCP, the balance between LMAF and HO might rather be tipped by pressure induced changes of the properties of URu_2Si_2 . This has for example been suggested in a recent proposal, where

HO and LMAF are believed to be variants of the same underlying complex order parameter [32]. In such a scenario, the HO is more likely to collapse at the proposed QCP as denoted by the dashed line (case II in Fig. 4). The pressure dependence of ΔC sets constraints on any theory of the HO involving quantum criticality.

In conclusion, using Larmor diffraction to determine the lattice constants and their distribution at high pressures and with very high precision, we were able to show that the SMAF in URu_2Si_2 is purely parasitic. Moreover, the HO and LMAF are separated by a line of first-order transitions ending in a bicritical point. This is the behavior expected for the HO being, e.g., incommensurate orbital currents, helicity order, or multipolar order.

We are grateful to P. Böni, A. Rosch, A. de Visser, K. Buchner, F. M. Grosche and G. G. Lonzarich for support and stimulating discussions. We thank FRMII for general support. CP and MV acknowledge support through DFG FOR 960 (Quantum phase transitions) and MV also acknowledges support through DFG SFB 608.

- [1] T. T. M. Palstra, et al., Phys. Rev. Lett. **55**, 2727 (1985).
- [2] M. B. Maple, et al., Phys. Rev. Lett. **56**, 185 (1986).
- [3] W. Schlabit, et al., Z. Phys. B **62**, 171 (1986).
- [4] C. Broholm, et al., Phys. Rev. Lett. **58**, 1467 (1987).
- [5] H. Amitsuka, et al., Phys. Rev. Lett. **83**, 5114 (1999).
- [6] L. P. Gor'kov and A. Sokol, Phys. Rev. Lett. **69**, 2586 (1992).
- [7] D. F. Agterberg and M. B. Walker, Phys. Rev. B **50**, 563 (1994).
- [8] N. Shah, et al., Phys. Rev. B **61**, 564 (2000).
- [9] V. P. Mineev, M. E. Zhitomirsky, Phys. Rev. B **72**, 014432 (2005).
- [10] P. Chandra, et al., Nature **417**, 831 (2002).
- [11] A. Kiss, P. Fazekas, Phys. Rev. B **71**, 054415 (2005).
- [12] C. M. Varma, L. Zhu, Phys. Rev. Lett. **96**, 036405 (2006).
- [13] F. Bourdarot, et al., Physica B **359-361**, 986 (2005).
- [14] G. Motoyama, et al., Phys. Rev. Lett. **90**, 166402 (2003).
- [15] S. Uemura, et al., J. Phys. Soc. Japan **74**, 2667 (2005).
- [16] E. Hassinger, et al., Phys. Rev. B **77**, 115117 (2008).
- [17] G. Motoyama, et al., J. Phys. Soc. Japan **77**, 123710 (2008).
- [18] H. Amitsuka, et al., J. Magn. Magn. Mat. **310**, 214 (2007).
- [19] K. Matsuda, et al., J. Phys.: Condens. Matter **15**, 2363 (2003).
- [20] M. Yokoyama, et al., Phys. Rev. B **72**, 214419 (2005).
- [21] P. G. Niklowitz, et al., Proceed. SCES 2008.
- [22] M. T. Rekveldt, et al., Eur. Phys. Lett. **54**, 342 (2001).
- [23] T. Keller, et al., Appl. Phys. A (Suppl.) **74**, 332 (2002).
- [24] C. Pfleiderer, et al., J. Phys. Condens. Matter **17**, S3111 (2005).
- [25] C. Pfleiderer, et al., Phys. Rev. B **74**, 104412 (2006).
- [26] C. Pfleiderer, et al., Science **316**, 1871 (2007).
- [27] A. de Visser, et al., Phys. Rev. B **34**, 8168 (1986).
- [28] T. Kagayama, et al., J. Alloy. Compd. **213**, 387 (1994).
- [29] A. Villaume, et al., Phys. Rev. B **78**, 012504 (2008).
- [30] S. Elgazzar, et al., Nat. Mater. **8**, 337 (2009).
- [31] C. R. Wiebe, et al., Nature Phys. **3**, 96 (2007).
- [32] K. Haule and G. Kotliar, arXiv:0907.3889 and 0907.3892.